communications biology

A Nature Portfolio journal

Article

Article in Press

https://doi.org/10.1038/s42003-026-10917-2

Deciphering the genomic signatures of climate vulnerability across 77 sheep breeds

Mario Barbato[1,2], Elia Vajana[3,4] ✉, Oliver Selmoni[4,5], Elisa Somenzi[2], John L. Williams[2], Oscar Cortés[6], Luís Telo da Gama[7], Alfredo Teixeira[8], Pablo Orozco-terWengel[9], Maria Trinidad Pérez Méndez[10], Anouk Schurink[11], Jack J. Windig[12], Sipke Joost Hiemstra[13], Linn Fenna Groeneveld[14], Gábor Mészáros[15], Eve Rannamäe[16], Urmas Saarma[17], Anneli Ärmpalu-Idvand[18], Anna M. Johansson[19], Paola Crepaldi[20], Antonello Carta[21], Tiziana Sechi[21], Badr Benjelloun[22], Gwenola Tosser-Klopp[23], Bertrand Servin[23], Michèle Tixier-Boichard[24], Stephane Joost[4], Barbara Lazzari[25], Alessandra Stella[25], Licia Colli[2,26], IMAGE Consortium* & Paolo Ajmone Marsan[2]

Among domesticated species, sheep (*Ovis aries*) have achieved a wide geographic distribution due to their mobility, rusticity and ability to adapt to diverse environments and climatic conditions. Here, we characterise the genome-wide diversity of >1,000 sheep representing 77 autochthonous breeds spanning North Africa to Scandinavia using high-density genotype data. To provide a large-scale assessment of population vulnerability to climate change, we combine uni- and multivariate gene-environment association analyses, and quantify the deviation of the current genomic make-up of populations from that necessary for maintaining adaptation under climate change (genomic offset). We identify precipitation as a major driver of divergent selection and identify candidate adaptive loci overlapping genes with pleiotropic roles linking renal water balance and metabolic regulation, including glucose and insulin-related pathways. This coupling of osmoregulatory and metabolic functions likely underpins adaptation to variable drought regimes and extreme, fluctuating environments. Notably, genomic offset hot spots are identified in southwestern Europe, highlighting the need for targeted management to mitigate the effects of climate change on animal welfare and production in these regions. These findings shed light on the strategies for climate adaptation in sheep and provide insights for informed breeding programmes aimed at enhancing resilience in changing climate conditions.

The global need for livestock products is predicted to double by 2050 due to the increasing human population and higher standards of living. Animal production will need to increase accordingly to meet the demand[1]. However, the effects of global climate change are expected to challenge the ability of livestock to cope with new environmental conditions, varying by geographic region and production type, threatening food security and ultimately reducing the performance of all agriculture from grazing to mixed farming and intensive systems[2].

Changes in precipitation patterns, relative humidity and heat stress have already become noticeable in livestock farming in temperate zones, affecting animal welfare, production efficiency and limiting biomass availability[1,3]. Moreover, higher lignin accumulation, lower protein content, and reduced forage digestibility ultimately contribute to a decline in energy yield[4,5]. The Mediterranean basin has been identified as one of the most vulnerable regions for climate change, with a predicted significant increase of average atmospheric temperature, annual thermal variability, increased drought especially during summer, and changed land-use[2].

Among livestock species, small ruminants such as sheep (*Ovis aries*, Linnaeus, 1758) are particularly sensitive to climate change, as they are typically reared in low-input production systems, and many of their physiological processes are influenced by local adaptation to seasonal fluctuations[6,7], that is, genetic differences between populations that confer a

A full list of affiliations appears at the end of the paper. *A list of authors and their affiliations appears at the end of the paper. ✉e-mail: eliavajana@cnr.it

selective advantage under specific regional environmental conditions[8]. As in other livestock species, the process of local adaptation to different climates in sheep began after the domestication from the wild ancestor, the Asiatic mouflon (*Ovis orientalis*, Gmelin, 1774), which occurred in the Fertile Crescent in the Early Neolithic[9]. Following domestication, sheep spread around the world as a result of human migration and trade[10], and were reared under different environmental, management, and selection conditions, leading to >1400 breeds adapted to a wide range of climates, pathogen challenges, and production systems[11]. Adaptation to local climatic conditions has ultimately enabled modern sheep to mitigate environmental stress, thereby enhancing the efficiency and sustainability of their production[2].

Local adaptation is driven by spatially divergent selection and genotype *x* environment interactions[8] that can be mediated by a few loci with large effects and/or many loci with small effects. Alleles at these loci may have opposite effects in different habitats (antagonistic pleiotropy) or confer optimal fitness in their own habitat, but have no effect elsewhere (conditional neutrality)[8,12]. Gene flow and genetic drift can influence local adaptation with the introgression of new beneficial variation from external populations (adaptive introgression) or the loss of advantageous variants[8,11].

From an evolutionary perspective, climate change involves a spatial shift in natural selection, threatening the balance between adaptive alleles and the environment, and causing maladaptation in animals adapted to specific habitats[13]. Genomic offset is a measure of genetic vulnerability to environmental change quantified as the distance between the current genetic composition and that required to maintain optimal fitness in a changing environment[14]. By assuming that adaptive loci mediate the effect of the environment on fitness, recent studies have reported climate change-related offsets based on genomic data and climate projections without direct trait measurements[12,15]. Even though they have been validated in several contexts (see, for example, Capblancq et al.[16]), offset metrics have rarely been used to inform the management of livestock genetic resources under climate change[17], despite their potential for conservation and the increased accuracy and availability of environmental and genomic databases[18]. In this context, local sheep breeds are particularly valuable for unravelling the genetic signature of local (mal)adaptation, due to their well-documented natural history, availability of well annotated genomes and genomic characterisation conducted across different geographical scales.

Identifying genes within candidate regions, from genome-wide selection scans has revealed both convergent and intraspecific adaptation to environmental stressors across several livestock species[19], including cattle adapted to tropical environments[20] and sheep reared at high-altitudes[21]. In this paper, we used this approach to explore a large, geo-referenced dataset containing genome-wide genotypes of local sheep populations representative of Europe, North Africa and West Asia. We identified the genetic factors involved in adaptive differentiation that may be responsible for environmental adaptation and quantify the expected, climate change-related genomic offset in these regions. Our results support the development of genome-informed strategies for adaptive management of locally adapted sheep populations.

Methods

Sampling, data production and quality control

Identifying loci under spatially divergent selection is challenging because several neutral evolutionary processes, such as genetic drift, allele surfing and gene flow, can generate deceptive signals across the genome, blurring genuine selection signatures[22]. In order to characterise adaptive variation specifically, ad hoc sampling strategies involving multiple populations that evolved in differentiated habitats are necessary. Key parameters for detecting adaptive variants include the geographic distribution of sampling locations, sample size, and genome-wide coverage[23]. To address these challenges, we used hierarchical clustering of principal components (HCPC; Supplementary Note 1) to guide the sampling of environmental variability (Fig. 1a). This approach was combined with extensive genome wide coverage (> 160,000 SNPs) and a large sample size ($n > 1000$ animals)[23]. A limitation of any prediction of genomic vulnerability to climate change is the implicit assumption that populations are close to their current local adaptive optimum, which may not always be true[15]; to mitigate this issue, our sampling focused on local breeds, typically maintained within the same environmental context for multiple generations and not subjected to intensive artificial selection.

This study was reviewed by the ethical committee (Organismo Preposto al Benessere Animale; OPBA) of the Università Cattolica del Sacro Cuore (Italy). The committee determined that the research met the criteria for exemption from formal animal research ethical approval (Doc 5 Parere OPBA_PC-R08-2026). A total of 962 geo-referenced sheep biological samples (blood, semen and extracted DNA) were provided by the EU IMAGE project (Innovative Management of Genetic Resources H2020: 677353) partners, covering most of the European territory, Morocco and northern Iran (Supplementary Fig. 1, Supplementary Tables 1 and 2). Total DNA was extracted using tissue-specific commercial kits, depending on the type of biological material. For blood samples, DNA extraction was performed using the GenElute™ Mammalian Genomic DNA Miniprep Kit (Sigma-Aldrich®) following the manufacturer's protocol. For semen samples, DNA was extracted using the NucleoSpin® Tissue kit (Macherey Nagel GmbH & Co., https://www.mn-net.com/) with a modified protocol (Supplementary Note 2).

Based on the quality of the extracted DNA, the breed of origin and the geographical provenance, a subset of 672 individuals was selected for genotyping using the Illumina Ovine Infinium® HD SNP BeadChip[24], which includes >600 k single nucleotide polymorphism (SNP) markers. A further 35 additional individuals were whole-genome sequenced using 150 bp paired-end reads on an Illumina platform, with sequencing outsourced to Novogene (https://www.novogene.com/). An average of 41 ± 5.5 Gb raw data were produced per sample, giving an average genome coverage of 12X per individual. Sequences were first trimmed with trimmomatic v.0.35[25] and mapped to the *O. aries* reference genome version Oar_v3.1 with BWA v.0.7.17[26]. Optical and PCR duplicates were identified and marked using Picard tools v.2.18.2[27], then local realignment around indels and base quality recalibration were done with GATK v.3.7.0[28] to improve variant concordance and to correct sequencing errors or other artefacts. Variants were independently called with three callers: GATK HaplotypeCaller, samtools mpileup v.1.8, bcftools v.1.6, and FreeBayes v.1.1.0[29]. After quality-control, HD genotypes were extracted from the list of variants called from WGS sequences and merged with HD genotype data, together with a set of 738 samples genotyped or sequenced that were made available by the IMAGE partners (Supplementary Table 1). These included two European mouflons (*Ovis gmelini*, Blyth, 1841) and 14 Asian mouflons (*O. orientalis orientalis*). The European mouflons were collected in southern France (Sigean Park) as descendants of mouflons from Bavella (Corsica)[30,31], while the 14 Asian mouflons were sampled in an area of northwestern Iran, likely corresponding to the cradle of sheep domestication, and were obtained from the European NextGen project (http://nextgen.epfl.ch/) as part of the NextGen consortium data sharing agreement[30,31]. The final HD dataset comprised 1,445 individual genotypic profiles. Marker positions were updated to the ARS-UI_Ramb_v2.0 sheep genome ref. 32.

PLINK v.1.9[33] was used to remove SNPs located on sex chromosomes, and those with unknown map positions, a call rate <95%, or minor allele frequency (MAF) < 1%. Pairwise genome-wide identity-by-descent (IBD) estimates were obtained using the method of moments in PLINK. To remove up to second-degree relationships, one individual from each pair with IBD > 0.08 was randomly removed. Linkage disequilibrium (LD) pruning was performed using the --indep-pairwise function, where SNPs with $r^2 > 0.2$ were randomly removed from sliding windows of 2000 kb and a step size of 200 kb.

Genetic structure

We investigated population genetic structure using an individual-based principal components analysis (PCA), constructing a population-based neighbour joining (NJ) tree, measuring Wright's pairwise fixation index

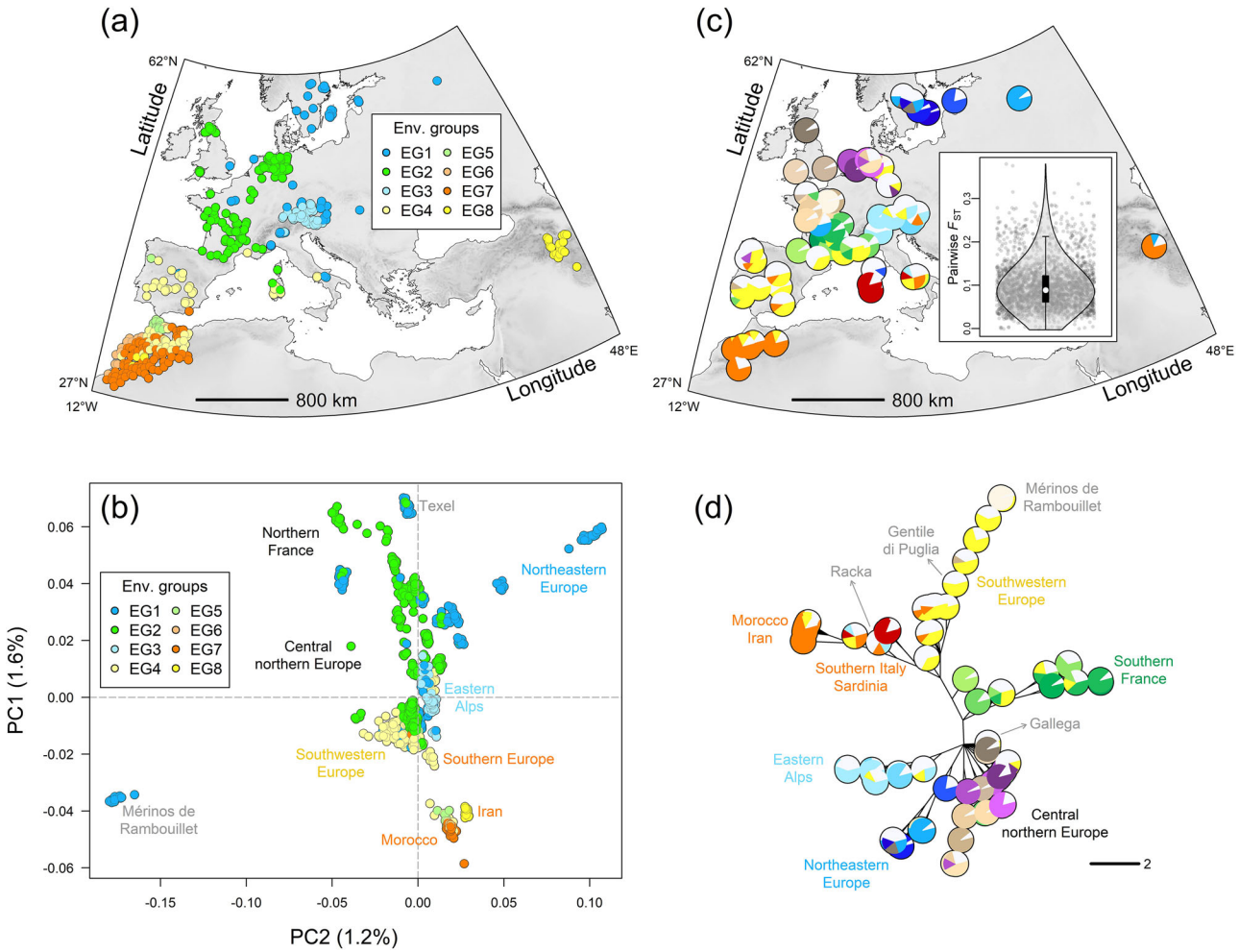

Fig. 1 | Sampling and population genetic structure. a Geographical distribution of the analysed sheep samples ($n = 1075$ animals). Individuals are shown by dots based on their sampling location. The colour key represents environmental clustering (EG: environmental group; see Supplementary Table 2). **b** Individual-based principal component analysis. Individuals are coloured as in panel (**a**). The principal component 1 (PC1: vertical axis) and 2 (PC2: horizontal axis) roughly order individuals by their geographical origin, with PC1 reflecting latitude and PC2 separating highly differentiated populations such as Mérinos de Rambouillet, and populations from northeastern Europe (Gotland and Gute). The scores on PC2 have been inverted for graphical purposes. **c** Admixture analysis presented on a geographical basis for the $K = 29$ model. Individual ancestries are averaged per population and presented as pie charts. The inset shows the distribution of pairwise F_{ST} ($n = 2{,}926$ comparisons), with the black point indicating the median (median pairwise $F_{ST} = 8.9\%$). **d** Phylogenetic relationship between populations inferred from a 90% bootstrap consensus NJ tree. The pie charts represent admixture proportions based on the $K = 29$ model. The southernmost populations are grouped along three main branches corresponding roughly to Iran, Morocco and Italy, Iberia and the Mediterranean France. Populations from the eastern Alps, northeastern Europe and central/northern Europe are on separate branches.

(F_{ST}), and testing for the presence of K ancestral gene pools using a sparse non-negative matrix factorisation algorithm (sNMF)[34]. We used the sNMF implementation provided by the LEA v.3.22.0 R package[35] assuming from $K = 1$ to 35 gene pools with 100 replicates per K, a regularisation parameter of 100, a tolerance error of 10^{-5}, and 200 iterations. We masked 5% of the genotypes to derive the cross-entropy of each replicate and relied on the mean cross-entropy decay to identify a plausible K (Supplementary Note 3). PCA was performed using the snpgdsPCA function from the SNPRelate v.1.44.0 R package[36]. The NJ tree was obtained based on pairwise Nei's distances using the R functions dist.prop from ade4 v.1.7.24[37] and nj from ape v.5.8.1[38]. The tree was rooted in the Asian mouflon population and bootstrapped 100 times using the boot.phylo function from ape[39]. Nodes with <90% support were collapsed. Breeds with fewer than five individuals were excluded from the calculation of genetic distances to avoid bias due to small sample sizes. Pairwise F_{ST} values were measured using the Hudson's method as implemented in PLINK v.2.0[33,40].

Environmental information

Values for altitude, 19 bioclimatic variables, monthly precipitation, and monthly minimum and maximum temperatures were retrieved for each sample from the Worldclim v.2.1 database at a resolution of 1 km^2 and a time span of 1970–2000[41]. Seasonal precipitation and seasonal minimum and maximum temperatures were derived by taking the median values of December, January and February (winter), March, April and May (spring), June, July and August (summer), September, October and November (autumn). To quantify heat stress, monthly relative humidity, mean temperature and diurnal temperature range were derived from the Climate Research Unit database v.2.0 at a resolution of ~340 km^2 and a time span of 1961–1990[42], and used to derive monthly values for the temperature-humidity index (THI). The average of the THI values in July and August (i.e., the months at highest heat stress in Europe) was added to the set of variables to be tested in GEA analysis, which gave an environmental matrix composed of 33 environmental variables. To quantify collinearity within the environmental matrix, we computed the Pearson's correlation coefficients (r) between all pairs of environmental variables, and deemed two variables

to be collinear when $|r|>0.7$[43]. To obtain a non-redundant environmental matrix, one variable per pair with $|r|>0.7$ was then randomly excluded before estimating GEAs. Given the existence of overlapping environmental gradients, we interpreted the retained variables as proxies for broader environmental signals rather than as uniquely informative predictors. This resulted in a reduced environmental matrix suitable for multivariate gene-environment association tests (see next section), while acknowledging that alternative variable selection strategies might retain predictors with greater biological interpretability and/or association with genetic gradients[16].

Gene-environment association analysis

A gene-environment association (GEA) analysis was used to identify candidate molecular signatures of local adaptation. To reduce the risk of false associations, we combined univariate (latent factor mixed models) and multivariate (partial redundancy analysis) GEA approaches, while taking into account neutral population structure, and considered SNPs common to both as candidate molecular signatures of selection[22,44].

We tested univariate genotype-environment associations using the LFMM 2 algorithm as implemented in the lfmm R package[45]. LFMM 2 is an efficient GEA analysis based on the simultaneous estimation of genotype-environment associations and a given number of N latent factors that model neutral genetic structure and correct for its confounding effect. In this approach, the selection of N can be guided by the sNMF analysis, the environment is treated as a fixed effect, and the regression coefficients quantify the relationship between the genetic markers and the environmental covariates. Under the null hypothesis of no relationship between genotype and environment, regression coefficients are assumed to be distributed following a Student distribution with $n-(N-1)$ degrees of freedom, n being the number of individuals in the test. Regularised least squares estimates of the effect sizes were obtained using the lfmm_ridge function. P-values were obtained using the lfmm_test function for all GEA tests, and calibrated using the genomic control method. Finally, false discovery rate (FDR) was tested separately for each environmental covariate by transforming p-values to q-values using the qvalue v.2.42.0 R package[46]. GEA tests were considered statistically significant at a nominal FDR cut-off of 1%, and missing genotypes were imputed prior to analysis using the 'mode' method, as implemented in the impute function from LEA.

We used partial redundancy analysis (pRDA) to complement LFMMs in screening the sheep genome for both mono- and polygenic signatures of local adaptation. Redundancy analysis is a constrained ordination procedure where the genomic and environmental matrices are simultaneously tested for association by means of a multi-response multiple linear regression followed by a PCA of the fitted values of the genotypes. As a result, the environmental matrix conditions the ordination axes, which model genomic variation throughout a linear combination of the focal environmental variables, and identify sets of genotypes covarying with the environment[47]. As LFMMs, pRDA allows the false discovery rate to be controlled by filtering out the effect of neutral genetic structure when estimating the gene environment relationship[16].

For consistency between univariate and multivariate testing, the latent variable score matrix was derived from the LFMM analysis and used within the pRDA model to correct for neutral genetic structure[45,48]. Environmental and population structure covariates were standardised prior to analysis and their collinearity was assessed by calculating pairwise Pearson's correlations: if redundant ($|r|>0.7$), covariates were excluded. The statistical significance of the model, including environmental covariates conditional on neutral population structure, was assessed using an F test based on 999 permutations of individual genotypic profiles under the null hypothesis of no linear relationship between the SNP and environmental matrices[47]. The canonical axes of interest were identified by inspecting the pRDA scree plot. A locus was considered putatively under divergent selection if its score on at least one canonical axis deviated from the mean by more than ± 3 SDs (two-tailed $p \le 2.7 \cdot 10^{-3}$)[16,44]. Partial RDA and permutation tests were performed with the rda and anova.cca functions, respectively, using the R package vegan v.2.6.10[49].

Gene annotation and GO analysis

For each significant locus identified by LFMMs or pRDA, genes within 20 kbp were selected, which corresponds to the approximate distance at which LD halves in sheep[50]. To understand the biological pathways represented by these candidate genes, a gene ontology (GO) enrichment analysis was performed using GeneCodis v.4[51]. The genes intercepted by the SNPs identified by both pRDA and LFMMs were compared against a background set of genes identified by all the SNPs available after quality pruning. The GO terms were determined using the annotation of a close species (*Bos taurus*, Linnaeus, 1758) and deemed significant for $p \le 0.05$ after Benjamini-Hochberg correction. Significant GO terms were aggregated for semantic similarity using GO-Figure! v.1.0.2[52].

Local genomic offset

We calculated an individual-based local genomic offset metric[53] in three steps: first, we derived an adaptive index reflecting the current adaptive genetic turnover, assuming equilibrium between allele frequencies and climatic conditions (which we refer to as the current adaptive landscape[16]); second, we calculated the expected shift in this index required to maintain optimal fitness in situ under future conditions (the future adaptive landscape), assuming no gene flow among populations[15]; finally, we quantified the mismatch between current and future adaptive landscapes as the difference between the current and future adaptive index at each location (pixel) in the study area[54].

To obtain the current adaptive landscape, we performed an adaptively enriched RDA using the individual genotypes of the SNP outliers common to both LFMMs and pRDA as the multivariate response and the set of standardised focal environmental variables as the explanatory matrix, without correction for neutral genetic structure[14,16]. Statistically significant ordination axes were identified using the F test implemented in the R function anova.cca[49], which evaluates the eigenvalue of each axis over 999 permutations, and a significance threshold of 0.01. The adaptive index was then derived separately for each significant axis and pixel of the landscape, as follows:

$$Adaptive\ index = \sum_{i=1}^{n} a_i b_i,$$

where a_i is the loading of environmental variable i along a given RDA axis and b_i is the standardised value of environmental variable i at a given pixel. To obtain a synthetic representation of the current adaptive landscape that conveys information from all significant axes, we used the derived indices in a K-means analysis to test for the existence of clusters of individuals with similar scores (adaptive groups[55]). We tested from 1 to 10 adaptive groups (K_a) and applied the average silhouette method to identify the best solution using the fviz_nbclust function from the factoextra v.2.1.0 R package[56].

To predict the future adaptive landscape, we used ACCESS-CM2, a hot-labelled global climate model (GCM) with an equilibrium climate sensitivity of approximately 4.7 °C[57], to determine the projected distribution of focal environmental variables at a 5 km² resolution for 2081–2100 (Supplementary Fig. 2)[58,59]. Projections were generated under Shared Socioeconomic Pathways (SSP) 2-4.5 and SSP5-8.5, representing moderate and severe climate change, respectively[60]. Then, we weighted these climate projections by the loadings of the adaptively enriched RDA, reflecting the strength of contemporary gene-environment relationship. Finally, we quantified local offsets as the Euclidean distance between current and future adaptive landscapes at each pixel[16]. For qualitative interpretation, local offset values were classified into four categories based on the quartiles of the offset distribution. To assess sensitivity to GCM choice, we repeated the genomic offset analysis using MIROC6, a more conservative model with an equilibrium climate sensitivity of 2.6 °C, alongside ACCESS-CM2, under SSP2-4.5 and SSP5-8.5 for the same time horizon (2081–2100).

To test whether the severe climate change scenario (SSP5-8.5) was associated with greater genomic vulnerability than the moderate scenario (SSP2-4.5), a paired-samples sign test was performed using the SIGN.test

function in the BSDA v.1.2.2 R package[61]. This test was applied after confirming that the differences in individual offsets were not normally distributed. To evaluate differences in mean genomic offset between adaptive groups, two-sample *t*-tests were performed for each climate change scenario, after verifying the homogeneity of variances assumption with Levene's test; *p*-values were adjusted for multiple testing using the Bonferroni correction.

A two-pronged strategy was used to characterise uncertainty in the offset estimates obtained from the adaptively enriched RDA. First, we identified and mapped areas where environmental values fell outside the range represented in the training data (the extrapolation areas). Local genomic offset estimates in these areas may be less reliable because they are based on a poorly characterised gene-environment relationship and are therefore more sensitive to model assumptions[62]. Second, we quantified agreement with an alternative modelling framework. Although the adaptively enriched RDA effectively captures orthogonal patterns of gene-environment covariation, it assumes linear relationship and may therefore oversimplify complex gene-environment associations[15]. We therefore fitted a Gradient Forest (GF) model using the same predictors and outlier loci to estimate current and future adaptive compositions and derived GF-based local genomic offsets under the same global climate model, climate scenario, and time horizon used for the RDA-based analysis[63]. Concordance between methods was assessed by comparing the quartile ranks across locations and classifying agreement as high, moderately high, moderately low, or low according to whether quartile differences were 0, 1, 2, or 3, respectively. GF analyses were performed with the gradientForest function from the gradientForest v.0.1.35 R package[64].

Finally, we assessed local spatial autocorrelation in offset values to identify spatial outliers and local clusters[65]. Animals with significantly higher or lower offset than their neighbours were classified as High-Low and Low-High outliers, respectively, while spatially proximate animals with consistently higher or lower offset than average formed High-High and Low-Low clusters, corresponding to hot and cold spots of local genomic offset. Local Moran's statistics were calculated for each animal using the mean RDA-based offset between SSP2-4.5 and SSP5-8.5, and *k*-nearest neighbours ranging between 5 and 100 to capture alternative combinations of neighbourhoods. Statistical significance was assessed using 999 conditional permutations, and pseudo *p*-values were adjusted for multiple testing using the Benjamini-Hochberg method at a 0.01 significance threshold. These analyses were performed with default settings using knn_weights and local_moran functions in the rgeoda v.0.1.1 R package[66].

Statistics and reproducibility

The analytical pipeline was implemented in R v.4.5.3[67,68]. Details of statistical analyses, including sample choice, algorithm parametrisation and software version, are reported in the relevant methods section. Figures 1a, b and 2a show 1075 of the 1112 animals analysed as 37 individuals had no environmental group assigned (Supplementary Data 1 and Supplementary Fig. 3). Statistical significance was marked with: ■$p < 0.1$, *$p < 0.05$, **$p < 0.01$, and ***$p < 0.001$.

Reporting summary

Further information on research design is available in the Nature Portfolio Reporting Summary linked to this article.

Results

Sampling, data production and quality control

Pruning for MAF, genotype and individual call rates, IBD, LD, and removing individuals with missing environmental information left the QC-ed dataset of 167,834 SNPs and 1112 individuals from 77 breeds (Supplementary Data 2). Eight environmental groups were identified by the HCPC analysis (Fig. 1a), ranging from cold, mesic zones in northeastern Europe and cool, temperate zones in central Europe, to extremely hot, xeric areas in southwestern Morocco[69] (Supplementary Table 2 and Supplementary Fig. 3).

Genetic structure

The PCA captured aspects of the genetic structure associated with geography (Fig. 1b). PC1, which explains 1.6% of the total genetic variation, orders individuals by latitude, and PC2 (1.2%) separates the highly differentiated populations from France (Mérinos de Rambouillet) and Sweden (Gotland and Gute breeds). The 32 largest PCs accounted for 15.2% of the total variation, which is consistent with the complex stratification known to occur in sheep populations[70]. Exploring the cross-entropy decay in the sNMF analysis revealed a minimum at $K = 29$ (Supplementary Fig. 4a). This corresponds to a complex mosaic of admixture and distinct gene pools throughout the European continent, consistent with the PCA (Fig. 1c). Particularly, a few spatially structured ancestral pools were identified in Iran and Morocco, southwestern Europe, the eastern Alps and northeastern Europe. In addition, most breeds from Great Britain (Scottish Blackface, Exmoor Horn and Suffolk), the Netherlands (Texel and Veluws Heideschaap), Sweden (Gotland and Gute) and central-northern France clustered into distinct genetic groups. In contrast, breeds showing consistently admixed ancestry were observed in Iberia, Germany, mainland Italy, Corsica, northeastern Europe (e.g., Rya), the eastern Alps (e.g., Racka), and France (e.g., Roussin de la Hague and the Romanov-admixed Romane[30,31]). The NJ tree mainly distinguished Iran, Morocco and southwestern Europe from central and northeastern Europe (Fig. 1d). Overall, genetic differentiation among populations was moderate, with mean pairwise $F_{ST} = 9.8\%$ (± 5%).

Gene-environment association analysis

As using too many latent factors can lead GEA models to overfit[71,72], we identified a parsimonious admixture model corresponding to $K = 10$ (see Supplementary Note 3 and Supplementary Fig. 4b), and hence used 10 latent factors to control for genetic stratification in both univariate and multivariate GEA models. To assess consistency in the representation of genetic structure across methods, we performed a Mantel test comparing individual genetic distances derived from ancestry coefficients at $K = 29$ (the optimal sNMF solution) with those derived from the 10 latent factors estimated by LFMM. This test yielded a positive and statistically significant correlation (Mantel R = 0.67, $p < 0.01$), indicating that the 10 latent factors captured genetic structure while preserving power to detect signals of selection (Supplementary Fig. 5 and Supplementary Note 4). Seven out of the original environmental variables were retained for GEA analysis after pruning the environmental matrix for collinearity (Table 1 and Supplementary Fig. 6).

Following LFMM analysis, a total of 75 SNP-environment associations involving 59 loci were found to be statistically significant at the 1% FDR cut-off (Supplementary Fig. 7). In particular, 23 and 22 loci were found to be associated with precipitation and temperature variables, respectively; four loci with both; six with altitude and temperature variables; two with altitude and precipitation variables; one with altitude; and one with autumn precipitation, isothermality and altitude (Supplementary Data 3).

No pathological collinearity was detected between the environmental and population structure covariates (Supplementary Fig. 8). The global pRDA model revealed a statistically significant relationship between the genomic and the environmental datasets ($F = 4.326$; $p < 0.01$). The focal environmental covariates explained an unbiased 1.9% genetic variation after correction for population structure. Inspection of the scree plot revealed that the first four canonical axes accounted for most of the genetic variance associated with the environment (1.5%; see inset in Fig. 2a). The first two canonical axes distinguished populations associated with high autumn rainfall, low isothermality and precipitation seasonality (central and northern Europe) from those associated with relatively high temperatures during the rainiest months of the year (summer in the eastern Alps and winter in southern Europe), high summer thermal minima (Morocco), as well as high precipitation seasonality, wide annual temperature ranges and living in mountainous environments (Iran; Fig. 2a). We found 1385 outliers on the first axis, 985 on the second axis, 940 on the third axis, and 965 on the fourth axis, for a total of 4275 SNP-environment associations with extreme

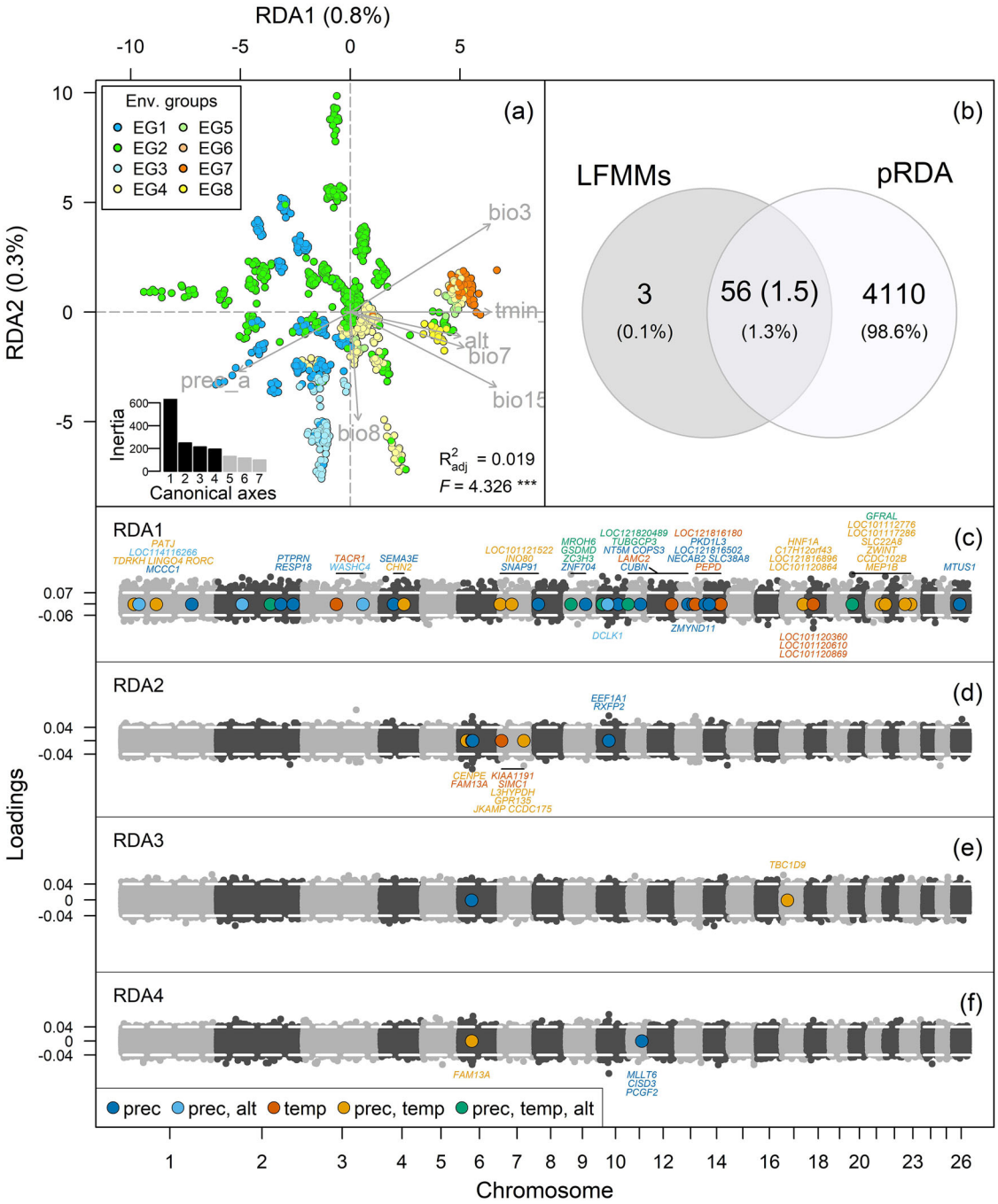

Fig. 2 | Gene-environment association analysis. a Triplot showing the ordination space defined by the first two canonical axes of pRDA. Individuals (n = 1075) are represented by coloured dots categorised according to their environmental group (EG; see Fig. 1a). Focal environmental predictors are shown as grey vectors (see Table 1 for abbreviations). The relative position of these entities reflects their relationship to the canonical axes, which are linear combinations of the environmental predictors. The angles between the SNPs and the environmental predictors, between the SNPs themselves, and between the environmental predictors themselves reflect their correlations. The pRDA scree plot is reported together with the unbiased amount of genetic variation explained by the model (adjusted R^2), the F statistic, and the proportion of genetic variation explained by the canonical axes (RDA1: 0.8%; RDA2: 0.3%). ***p-value < 0.001. **b** Venn diagram showing the number of SNPs found jointly by LFMMs and pRDA (overlap), and the number of SNPs found uniquely by each analysis. The expected random overlap is shown in brackets next to the observed overlap. The proportion of SNPs found in each subset is given as a percentage of the total number of significant results. **c–f** Manhattan plots showing the distribution of SNP loadings from the first four pRDA canonical axes. Loadings are referenced to the corresponding physical position along the sheep genome, with horizontal dashed lines indicating ± 3 SDs from the axis mean. SNPs that are intercepted by both LFMMs and pRDA are shown as square dots at their respective positions along the genome and are coloured according to the type of SNP-environment relationship (prec: precipitation-related variables; temp: temperature-related variables; alt: altitude). Genes physically associated with the outlier SNPs (i.e., candidate genes) are also shown and coloured accordingly.

Table 1 | Focal environmental variables retained after collinearity pruning

Focal environmental variable	Description	Pearson's correlation >|0.7|
prec_a - Precipitation in autumn (mm)	Median value of the average monthly precipitation in September, October and November	Annual precipitation (0.91), precipitation of wettest quarter (0.84) and month (0.84), precipitation in spring (0.80), precipitation of coldest quarter (0.78), precipitation in winter (0.77)
tmin_s - Minimum temperature in summer (°C)	Median value of the average minimum temperatures in June, July and August	Mean temperature of warmest quarter (0.94), annual mean temperature (0.93), minimum temperature in autumn (0.92), minimum temperature in spring (0.90), maximum temperature in autumn (0.88), maximum temperature in summer (0.84), THI (0.84), maximum temperature in winter (0.84), maximum temperature of warmest month (0.84), mean temperature of coldest quarter (0.83), maximum temperature in spring (0.82), mean temperature of driest quarter (0.80), maximum temperature in winter (0.76), precipitation in summer (0.75), precipitation of warmest quarter (0.75), maximum temperature of coldest month (0.72)
bio3 - Isothermality (%)	Ratio between mean diurnal range to the annual temperature range. It quantifies how large the day-to-night temperatures oscillate relative to the summer-to-winter (annual) oscillations	–
bio7 - Annual temperature range (°C)	Difference between the maximum temperature of warmest month and the minimum temperature of coldest month	Temperature seasonality (0.80), mean diurnal range (0.79)
bio8 - Mean temperature of wettest quarter (°C)	Average temperature in the four wettest months of the year	–
bio15 - Precipitation seasonality (percentage)	A measure of the variation in monthly precipitation over the year	Precipitation of driest quarter (0.82), precipitation of driest month (0.81)
alt - Altitude (m a.s.l.)	Elevation as derived from the Shuttle Radar Topography Mission (SRTM) elevation data	–

For each retained variable, a brief description and the most correlated variables are provided. The environmental information was derived at a resolution of 1 km^2, with climatic variables spanning the time period from 1970 to 2000. Mean diurnal range is defined as the mean difference between the monthly maximum and the monthly minimum temperature (°C). Temperature seasonality is defined as the standard deviation of monthly temperature averages (°C).

loadings (Supplementary Data 4). Specifically, 50%, 46%, and 4% of these associations were linked to temperature, precipitation, and topography variables, respectively, with 109 SNPs showing correlation across multiple axes. As a result, 4166 unique SNP outliers were detected.

We identified a statistically significant overlap of 56 candidate signatures of local adaptation between LFMMs and pRDA (Fig. 2b), accounting for approximately 1.3% and 95% of the SNP outliers found by pRDA and LFMMs, respectively. Among these shared candidates, 40 intercepted 63 genes across 20 chromosomes (Fig. 2c–f and Table 2).

Local genomic offset

The adaptively enriched RDA was statistically significant ($F = 88.352$; $p < 0.01$), with the focal environmental predictors explaining an unbiased 35.5% of genetic variation (Fig. 3a). The first canonical axis (explaining 30.6% of the total variance) contrasted individuals reared in mountainous areas with low autumn precipitation, high summer minima, high annual temperature range and high precipitation seasonality—a combination of conditions found in the Atlas Mountains of Morocco and the northern Zagros Mountains of Iran—with individuals experiencing higher autumn precipitation as well as lower summer minima and precipitation seasonality (continental and northern Europe; Supplementary Fig. 9). The second canonical axis (2.2%) may reflect an adaptive gradient from areas of high isothermality and low precipitation seasonality (e.g., the Atlantic coasts of Spain, France and Great Britain) to areas of higher precipitation seasonality (e.g., northern Morocco, southwestern Iberia, insular Italy and Iran).

We found six significant canonical axes and consequently calculated six adaptive landscapes that clustered into two main adaptive groups (Fig. 3b, Supplementary Fig. 10). The first group mainly comprised the European continent (adaptive group 1), while the second comprised North Africa, southwestern Iberia, and western Asia (adaptive group 2).

With local offsets ranging from 1.52 to 2.16, the Iberian and southwestern French breeds showed a moderately high genomic vulnerability under the SSP2-4.5 scenario (Fig. 3c). All other populations, with a few exceptions in northeastern France, showed a low (< 1.29) to moderately low (< 1.52) local offset. In the SSP5-8.5 scenario (Fig. 3d), most sheep from Iberia, France, Italy, northern Germany and Iran showed a high local offset (≥ 2.16) and those from inland Morocco, the eastern Alps, the Netherlands, southern England and Sweden showed a moderately high local offset (≥ 1.52). In contrast, the northernmost breeds from Great Britain and Sweden, Russia and southwestern sheep from Morocco showed moderately low (< 1.52) to low (< 1.29) local offsets.

With median values of 1.31 and 2.16, respectively, local offset under the SSP2-4.5 scenario was significantly lower than under the SSP5-8.5 scenario (p-value < 0.001; see inset in Fig. 3d). Under the SSP5-8.5 scenario, genomic vulnerability was statistically higher in adaptive group 1 than adaptive group 2, with mean values of 2.13 and 1.94, respectively ($t = 6.024$; $p < 0.001$). Under the SSP2-4.5 scenario, the difference between adaptive groups was only marginally significant, with adaptive group 1 showing slightly higher genomic vulnerability than adaptive group 2 (means = 1.29 and 1.25, respectively; $t = 2.161$, $p < 0.1$). The main patterns of genomic offset were broadly consistent across GCMs, with MIROC6-based estimates positively correlated with those obtained using ACCESS-CM2 (SSP2-4.5: $r = 0.71$; SSP5-8.5: $r = 0.76$; Supplementary Fig. 11).

Areas in which at least one environmental variable fell outside the ranges used for model training were identified and mapped (Fig. 1b–d and Supplementary Fig. 12). There was good convergence in offset ranking between RDA and GF models, with moderately high to high agreement observed at over 80% of sampling sites (Fig. 3c, d, Supplementary Fig. 13). Good model agreement and an absence of extrapolation were found to co-occur widely across the sampling locations, regardless of the climate change scenario considered. However, low levels of agreement were observed in certain locations, including central France, northwestern and southern Iberia, northern and southern Morocco, and southern Italy, depending on the climate change scenario considered.

Spatial autocorrelation analysis revealed a significant hot spot of genomic vulnerability in southwestern Europe, independent of the number of k-nearest neighbours used (Supplementary Fig. 14), which included most breeds from Iberia and central-southern France (Fig. 4 and Supplementary Table 3). In contrast, cold spots of genomic vulnerability were consistently identified in the eastern Alps, northeastern Europe, Great Britain, the

Table 2 | Genes associated with focal environmental variables (FDR < 0.01) identified by both LFMMs and pRDA

Chr	bp	Env-pRDA	Env-LFMM	FDR	Gene
1	37,131,323	bio15	bio3	1.98E-03	*PATJ*
1	51,267,576	bio15	bio3, alt	7.10E-03	*LOC114116266*
1	101,731,592	bio15	bio3	6.66E-03	*TDRKH, LINGO4, RORC*
1	204,833,508	prec_a	prec_a	1.54E-03	*MCCC1*
2	221,268,162	prec_a	prec_a	5.97E-03	*PTPRN, RESP18*
3	96,822,339	bio3	bio3	1.65E-03	*TACR1*
3	174,257,898	bio15	prec_a, alt	3.13E-04	*WASHC4*
4	38,509,974	prec_a	prec_a	2.38E-03	*SEMA3E*
4	68,288,042	prec_a	prec_a, bio3	4.08E-03	*CHN2*
6	22,061,519	bio3	bio3, bio15	2.84E-09	*CENPE*
6	36,395,849	tmin_s	prec_a	3.71E-03	*FAM13A*
6	36,593,100	bio3	bio3	1.75E-04	*FAM13A*
7	876,405	bio15	tmin_s	4.17E-03	*LOC101121522*
7	4,992,835	bio3	bio3	3.33E-03	*KIAA1191, SIMC1*
7	34,769,772	bio15	bio3	7.16E-03	*INO80*
7	69,816,226	bio3	bio3, bio15	9.90E-12	*L3HYPDH, GPR135, JKAMP, CCDC175*
8	10,803,163	prec_a	prec_a	4.25E-05	*SNAP91*
9	14,115,101	bio15	bio3, alt	7.80E-05	*MROH6, GSDMD, ZC3H3*
9	56,917,723	prec_a	prec_a	1.38E-03	*ZNF704*
10	29,501,536	bio15	bio15	2.73E-12	*EEF1A1, RXFP2*
10	25,887,743	bio15	alt	5.36E-03	*DCLK1*
10	85,530,224	bio15	bio3, alt	7.16E-03	*LOC121820489, TUBGCP3*
11	34,640,315	bio15	prec_a	7.72E-03	*NT5M, COPS3*
11	39,081,088	bio15	bio15	3.30E-06	*MLLT6, CISD3, PCGF2*
12	63,647,235	bio3	bio3	9.29E-03	*LAMC2*
13	30,799,248	bio15	prec_a	2.97E-03	*CUBN*
13	46,458,300	bio15	bio15	1.80E-03	*ZMYND11*
13	53,067,031	bio3	bio3	1.91E-05	*LOC121816180*
14	9,880,583	prec_a	prec_a	5.77E-03	*NECAB2, SLC38A8*
14	38,670,481	prec_a	prec_a	8.05E-03	*PKD1L3, LOC121816502*
14	43,367,948	bio3	bio3	1.19E-04	*PEPD*
17	17,101,279	bio8	bio8	4.08E-03	*TBC1D9*
17	63,325,817	bio15	bio3	3.71E-03	*HNF1A, C17H12orf43, LOC121816896, LOC101120864*
18	19,454,638	tmin_s	tmin_s	1.10E-11	*LOC101120360, LOC101120610, LOC101120869*
20	5,239,307	bio15	bio3, alt, tmin_s	4.43E-06	*GFRAL*
21	37,813,552	prec_a	bio3	7.41E-04	*LOC101112776, LOC101117286, SLC22A8*
22	2,539,883	bio15	bio3	6.06E-04	*ZWINT*
23	8,583,226	bio15	bio3	3.71E-03	*CCDC102B*
23	25,334,892	bio15	bio3	6.66E-03	*MEP1B*
26	18,682,085	prec_a	prec_a	1.54E-03	*MTUS1*

Chromosome (Chr) and physical position (bp) are reported based on the Rambouillet v.2 reference genome. The Env-pRDA and Env-LFMM columns list the environmental variables associated with each SNP position.

Netherlands and southwestern Morocco. Continental Italian breeds entered the hot spot for more than *k*-10 nearest neighbours, Iranian sheep were High-Low outliers for more than *k*-25 nearest neighbours, and significant High-Low outliers occurred for *k*-100 nearest neighbours in northeastern Morocco, possibly indicating vulnerable local populations; isolated Low-High outliers occurred in southwestern Iberia (Campaniça and Segureña) as well as France for more than *k*-20 nearest neighbours (Supplementary Fig. 14).

Gene annotation and GO analysis

The GO analysis identified 34 significant pathways involving 17 genes (Supplementary Data 5). Among them, the Hepatic transcription factor 1 homeobox A (*HNF1A*), the Protein Tyrosine Phosphatase Receptor Type N (*PTPRN*), and the PHD Finger Containing (*MLLT6*) contributed to 10, 7 and 5 terms, respectively, and were all associated with precipitation related variables, namely: *HNF1A* and *MLLT6* with precipitation seasonality (bio15), and *PTPRN* with precipitation in autumn (prec_a; Table 2). *HNF1A* is mainly expressed in the liver, gut, pancreas, and kidneys, where it

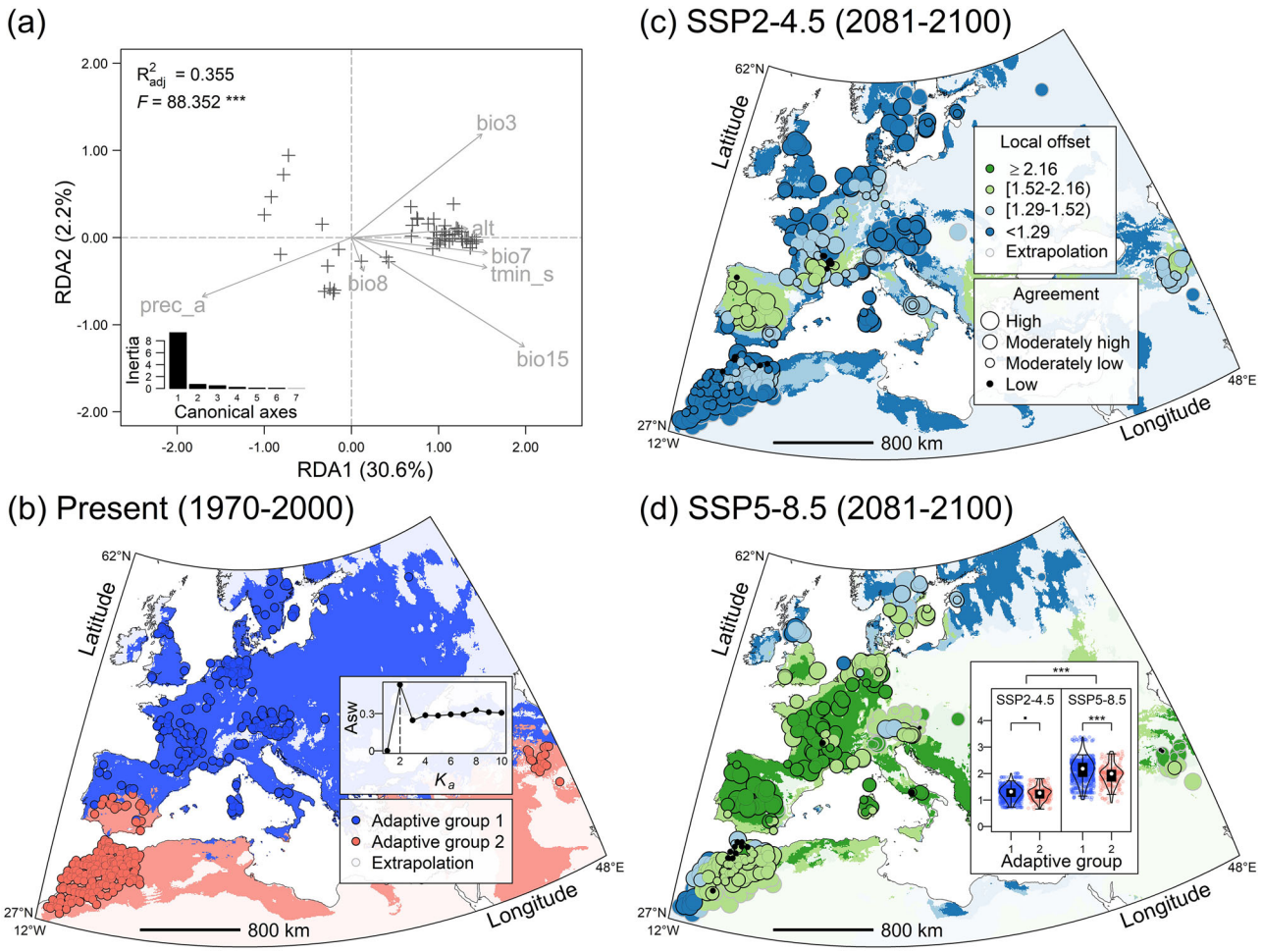

Fig. 3 | Local genomic offset. a Redundancy analysis biplot showing the association between the 56 outlier SNPs (crosses) and the focal environmental variables (vectors) in the adaptively enriched genetic space (see Table 1 for abbreviations). The angles between SNPs and environmental variables, and between SNPs or environmental variables themselves, reflect their correlation. The analysis resulted in seven ordination axes, six of which were found to be statistically significant (p-value < 0.01). **b** The current adaptive landscape, resulting from the adaptively enriched RDA model and subsequent clustering analysis of adaptive indices. The average silhouette width (Asw) identified two major clusters, one grouping individuals from Europe (adaptive group 1; n = 885 animals) and one grouping individuals from southwestern Iberia, Morocco and Iran (adaptive group 2; n = 227 animals). **c**, **d** Show the predicted local genomic offset for 2081-2100 based on a moderate (SSP2-4.5) and a severe (SSP5-8.5) climate change scenario, respectively. Four classes of genomic vulnerability were defined based on quartiles of the offset distribution and displayed using a colour key from dark blue (low offset) to dark green (high offset). Extrapolation areas are masked. Point size is proportional to the degree of agreement between redundancy analysis and gradient forest predictions. The inset in (**d**) shows the comparisons between climate change scenarios (paired-samples sign test), and between adaptive groups within each scenario (two-sample t-test) ***p-value < 0.001; ■p < 0.1.

contributes to regulating lipid and protein synthesis, water absorption, insulin secretion and glucose reabsorption[73]. Associations with feed efficiency and lipid metabolism have been described in cattle[74], whereas associations with fat deposition have been described in pigs[75]. *PTPRN* is a gene encoding the type I transmembrane protein primarily expressed in neuroendocrine cells such as pancreatic β cells, pituitary corticotrophs, and melanotrophs[76]. It is involved in insulin secretion and β-cell proliferation in the pancreas[77], and known to play a crucial role in neuroendocrine processes, including the regulation of secretion pathways, exocytosis, and hormone content modulation[76,78]. The *MLLT6* gene (or *Af17*) encodes a pivotal transcription factor increasing the expression of epithelial sodium channel (ENaC) genes and plays a vital role in salt and water reabsorption across various tissues[79]. This regulatory role contributes to maintaining electrolyte balance and proper hydration levels in the body.

Distinct clusters of semantic similarity were found for the significant GO terms from a scatter plot created using a method that minimises redundancy on semantic similarity (Fig. 5). Notably, one cluster encompassed renal potassium excretion and negative regulation of urine volume. Another cluster featured cobalamin transport and glucose import, while a separate group pointed to regulation of macrophage chemotaxis and regulation of DNA damage response. Additionally, we observed a cluster consisting of dense core granule maturation, Spemann organiser formation, and chromatin remodelling (Fig. 5 and Supplementary Data 6).

Discussion

Climate change is affecting both extensive and intensive livestock systems by altering key selective pressures across global agroecosystems. Breed vulnerability depends not only on the rate of environmental change and the population adaptive capacity, such as standing variation and phenotypic plasticity, but also on the extent to which management can buffer climatic stress. In many commercial breeds, productivity-driven selection may have reduced genetic diversity and increased sensitivity to environmental and nutritional fluctuations[80]. In sheep, where production systems are often low-input and management buffering may be limited, such vulnerability may be especially exposed. Conversely, local breeds are generally better adapted to the environmental conditions of their native regions, but this does not necessarily make them less vulnerable to future climate change. Their resilience may be compromised if rapid environmental change disrupts the

delicate gene-environment relationship on which local adaptation depends, particularly in systems with limited management intervention[6,19]. At the same time, local breeds may retain standing genetic variation associated with adaptation to heterogeneous or marginal environments, which could support rapid adaptive responses. Whether this reduced climate vulnerability depends on demographic conditions, management context, and whether environmental change proceeds faster than population adaptive capacity.

Univariate and multivariate GEA analyses (LFMMs and pRDA), which are robust to sampling design and statistical error, were combined to detect SNP-environment associations potentially involved in local adaptation across a wide range of local sheep populations from West Asia, Morocco, and Europe. Population stratification is a well-recognised challenge in this framework, as neutral genetic variation can produce spurious associations, leading to incorrect inference about loci involved in adaptation[22]. In our study, we observed a clear population stratification, with distinct gene pools (Fig. 1b), approximately 10% of genetic variance explained by population structure (Fig. 1c), and six main genetic groups corresponding to geographic origin (Fig. 1d). Cross-entropy analysis further suggested that the sampled populations derived from a mixture of 29 theoretical ancestral gene pools (Fig. 1c and Supplementary Fig. 4a), consistent with the complex evolutionary history of European sheep[70,81]. To account for this complexity while maintaining statistical power, we adopted a parsimonious admixture model of population structure in the GEA tests using ten latent factors (Supplementary Fig. 4b, Supplementary Fig. 5 and Supplementary Note 4).

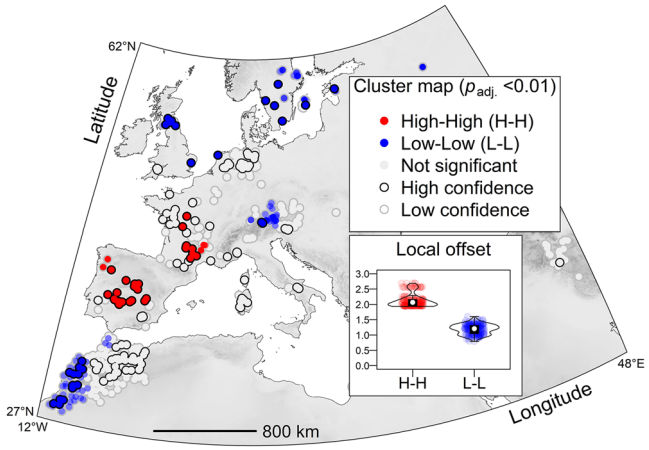

Fig. 4 | Cluster map of local genomic offset values. Cluster map of statistically significant hot and cold spots of projected genomic vulnerability for 2081–2100, based on *k*-10 nearest neighbours (High-High and Low-Low local clusters). Hot spots (red dots; $n = 165$ animals) have a median offset of 2.07, whereas cold spots (blue dots; $n = 188$ animals) have a median offset of 1.21. Non-significant locations (white dots; $n = 759$ animals) indicate no geographic dependence on the genomic offset. Breeds occurring within hot spots are found in Spain (Gallega, Spanish Merino, Colmenareña, Rubia del Molar, Manchega), Portugal (Churra do Minho, Churra da Terra Quente) and France (Causse du Lot, Charmoise, Blanche du Massif Central, Meat Lacaune, Romane, Dairy Lacaune, and Noire du Velay). Conversely, breeds within cold spots are mainly found in northern/northeastern Europe, the eastern Alps and southwestern Morocco (Supplementary Table 3). High-confidence sampling locations ($n = 245$ animals) were defined as those showing no extrapolation and moderately high to high agreement between the redundancy analysis and the gradient forest models under both climate change scenarios.

The 56 SNP outliers that were significant in both LFMMs and pRDA allowed to explain tenfold more genetic variance attributable to the environment than the full set of loci (25.3% versus 1.9%; Supplementary Table 4), minimised the false discovery rate within the outlier set[44], and were physically associated with 63 candidate genes (Table 2 and Fig. 2c–f). These genes were linked predominantly to precipitation-related variables, consistent with previous studies describing precipitation patterns, rather than temperature, as the main driver for global livestock selection[82]. Most associations with temperature-related variables involved isothermality, an index of annual thermal stability, and summer minimum temperature. The latter was highly correlated with THI ($r = 0.84$; Table 1), making it a reliable proxy for heat-stress variation across the study area, and isothermality has already been described as a selective driver in sheep[83]. This finding suggests seasonal thermal fluctuation as a major determinant of adaptive differentiation between climatically stable regions, such as the coasts of southern Europe and Mediterranean islands, and regions characterised by marked seasonality, such as northeastern Europe and the Alps.

The stringent focus on overlapping loci excluded over 4000 outliers that may contribute to multilocus local adaptation, thereby potentially biasing our results toward large-effect loci while overlooking the broader, more complex polygenic component of adaptation (Fig. 2b; see Forester et al.[44]). A broader examination of this extensive set of loci, combined with less conservative adjustments for genetic structure in GEA analyses, could serve as an alternative approach to reduce false-negative rates in future studies[15]. In addition, given the complex demographic history of sheep, future work might explicitly test the contribution of adaptive introgression as a source of adaptive variation. Repeated admixture and genetic exchange associated with migration, trade, and breed formation may have introduced alleles that were subsequently favoured under local environmental stressors. Integrating genome-scan approaches with analyses of admixture and

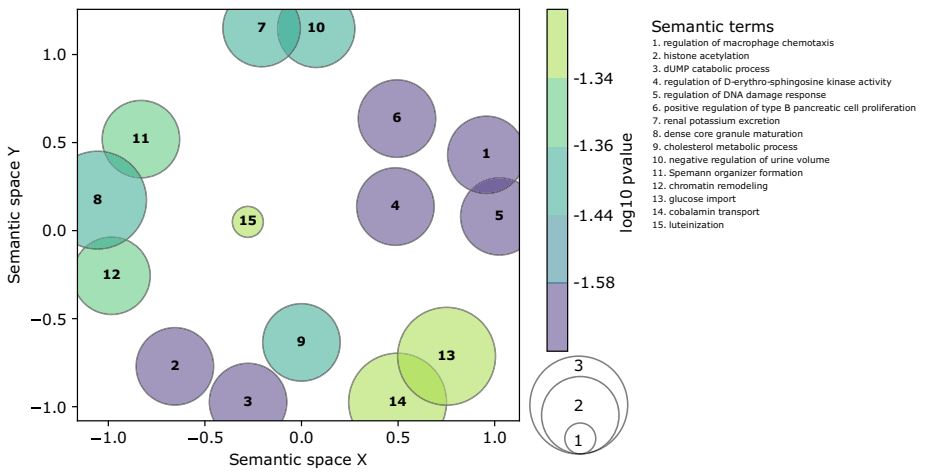

Fig. 5 | Semantic similarity analysis. Semantic similarity representation of the GO terms intercepted by the genes shared between LFMM and pRDA analysis. The numbers within each circle refer to a specific semantic term (see inset legend). Circle size reflects the number of GO terms in each group. Colours represent the *p*-value on a base 10 logarithmic scale. Only significant terms are shown.

introgression could therefore provide a more complete picture of the evolutionary processes shaping sheep adaptation.

Limited concordance exists in GEA studies in sheep[84], and most genes identified in this study have not been consistently implicated in environmental adaptation[6,11,85–87]. The exception is the *RXFP2* gene, a key determinant of horn morphology in ruminants[70,88,89] which was selected for during post-Chalcolithic sheep domestication[9]. *RXFP2* was also associated with morphological adaptation to harsh climates in sheep[90] and transcriptome differences between heat-tolerant and heat-susceptible pigs[91], suggesting additional adaptive roles beyond horn development. Moreover, genes hitchhiking with *RXFP2*, such as *EEF1A1* (Table 2), may contribute to metabolic pathways involved in adaptation. Higher concordance across studies is observed at the functional level, with genes often participating in similar metabolic pathways. The 34 significant GO terms identified were grouped into 15 clusters (Fig. 5), which we suggest represent four key environmental adaptation strategies: (i) water balance, (ii) metabolic adaptation, (iii) thermoregulation and stress response, and iv) reproductive adaptation. These strategies have cellular- to whole-organism implications (Supplementary Note 5).

We further examined how vulnerable the studied sheep populations are to climate change over the next six to eight decades. We quantified the local genomic offset of each population by measuring the difference between their current adaptive genetic makeup and the predicted optimal genetic composition under future climate conditions[15]. While we did not formally quantify the current degree of local adaptation (see, for example, Lotterhos, 2023[92]), the offset models used here are supported by prior evidence of locally adapted sheep in the study area[6,11,93], which is a key prerequisite for reliable offset estimations. Furthermore, the methodology employed (i.e., a redundancy analysis predicting adaptive genetic turnover based on environmental information) has been demonstrated to effectively predict genomic vulnerability in systems exhibiting high local adaptation within a stepping-stone framework[94], which is analogous to the dispersal mode of sheep during the Neolithic period[95].

Our estimates of local genomic offset were consistently greater than zero, even under the mildest emission pathway considered, suggesting that the analysed local breeds may be exposed to widespread vulnerability to future climate challenges (Fig. 3c, d). We found significant spatial dependence in local genomic offset values (Fig. 4), reflecting the combined effects of spatial turnover in adaptive genetic variation, projected local environmental changes, and the geographic distribution of sampling sites, which ultimately determines how neighbouring sites are defined[65]. Local breeds from Iberia and southwestern France were found to cluster within a hot spot of genomic vulnerability, whereas breeds from southwestern Morocco, the eastern Alps, the United Kingdom, and northeastern Europe were found to be located within cold spots of climate vulnerability (Supplementary Table 3). The effect of the sampling scheme was evident in Iran and northeastern Morocco, the most densely sampled areas, where a spatial discontinuity of high/low genomic offset emerged when analysing ≥15 nearest neighbours, identifying such populations as regional targets for genetic monitoring (Supplementary Fig. 14). On average, the climatic distance between present and future conditions was significantly greater in hot spots than in cold spots ($t = 4.41$, $p < 0.01$), but similar levels of climatic challenge were found to be associated with individuals with both low and high genomic vulnerability (Supplementary Fig. 15). These findings, together with the higher level of offset observed for the severe emission pathway (Fig. 3d), point to the key role of the degree of environmental change in determining the expected offset, while suggesting that comparable climatic shifts can result in different degrees of genomic vulnerability, depending on the sensitivity of local genotypes and/or the occurrence of pre-adaptive variation protecting against climatic stress (Supplementary Fig. 16). Consistent with this interpretation, the climatic variables contributing most to projected offset suggest that sheep local adaptation may be threatened by increasing heat, wider annual temperature ranges and greater autumn dryness, with potential downstream consequences for heat stress and animal diet (Supplementary Fig. 2). Importantly, although genomic offset estimates are expected to show some sensitivity to the choice of GCM, the overall agreement between ACCESS-CM2- and MIROC6-based results suggests that the main biological patterns identified here are robust to GCM selection. A more detailed sensitivity analysis, incorporating multiple GCMs, could reveal discrepancies in offset estimates across spatial scales, improve understanding of model uncertainty, and define a range of genomic vulnerabilities across locations, hence helping refine management intervention priorities.

The adaptive landscapes obtained, and consequently our offset models, lack a standardised metric. This complicates the biological interpretation of our offset predictions and limits their application to the populations analysed, preventing direct comparisons with other studies. However, calculating the contemporary spatial offset, i.e., the offset populations would experience if relocated from their current breeding sites, enables us to identify where future offsets would manifest under present conditions, providing a geographical perspective of the phenomenon and serving as an indirect measure of the severity of our predictions[96]. Using this approach, we found that an increase of one unit in spatial offset corresponds, on average, to a movement of 1.3 degrees of longitude (~145 km east-west) and 2.2 degrees of latitude (~278 km north-south) from the current breeding sites. For instance, Spanish Merino sheep would need to be displaced approximately 760 km north from their current location in southwestern Spain to achieve the expected genomic offset of 2.2 by 2081–2100 (Supplementary Table 3). Similarly, the Gute sheep would require a southward relocation of about 380 km from southern Sweden to reach the expected offset of 1.2 by the same period. This would correspond to raising Spanish Merino in the Vendée region of northwestern France, and Gute sheep along the Polish coast. While these examples are effective, they are based on a model that does not consider environmental factors other than climate, ignoring cues that can be relevant in affecting fitness during latitudinal relocation, as reported on the effect of photoperiod on reproductive fitness[97]. Explicit relocation models would be required to account for the relationship between genetic variation and factors such as day length or local solar radiation.

Although imperfect, the individual rankings of offset values obtained using adaptively enriched RDA and GF showed good agreement (Supplementary Fig. 13). Together with the identification of extrapolation areas and the strong convergence obtained across different GCMs (Supplementary Fig. 11), this result suggests that the proposed offset model is broadly reliable, although its biological validity in management contexts ultimately depends on empirical validation. This step is especially complex in livestock systems, where adaptive responses are also shaped by factors such as management and heterogeneous production environments, including variation in feed resources and disease challenge[98]. Agreement among location rankings produced by different offset approaches is known to be highly variable, ranging from substantial convergence[99] to no correlation or marked discordance among methods[100,101]. This variability may reflect case-study-specific effects linked to demographic history and genotyping strategy, as well as technical factors related to modelling assumptions, including the nature of the relationship between genetic and climatic gradients[100,101]. Here, we found contrasting rankings for groups of individuals located in northern Morocco and central-southern France (Fig. 3c, d), highlighting areas where deviations from assumed Gaussian selection and/or linear genotype-environment relationship may occur[16]. The greatest environmental novelty was found in under-sampled regions, particularly northeastern Africa and eastern Europe (Supplementary Fig. 12). This requires extreme caution when interpreting offset values in these regions and highlights the need for future research to address this sampling gap.

Our analysis of local sheep breeds from diverse environments across Europe, Morocco and Iran, revealed precipitation as a predominant selective force. Regulatory genes such as *HNF1A*, *CUBN*, and *MLLT6* were identified, highlighting pleiotropy as a central adaptive strategy to climatic pressures. This gene action likely facilitates the optimisation of interconnected physiological systems, enhancing resilience to environmental fluctuations. These findings suggest that adaptive processes for water balance, metabolic functions, thermoregulation, and reproduction often

involve convergent gene sets, despite limited overlap among studies on environmental adaptation.

In light of rapid genetic loss in agroecosystems, we advocate for future research into genomic offset metrics and their integration with established indicators like Ne 500 and PM, in order to monitor the genetic status of livestock populations[102,103]. This tool can add further information to characterise genomic vulnerability, aiding conservation prioritisation and guiding strategies such as in situ conservation, breed replacement, or the introduction of preadapted variation through breeding programmes. This is particularly important when genetic erosion is rapid and the species in question, such as sheep, represents a key resource for rural communities.

Examining spatial and spatio-temporal offsets may help predict areas where future conditions will align with current spatial offsets, facilitating the establishment of evolutionary rescue networks. These networks could promote genetic exchange between donor and recipient populations, while minimising disruption to local adaptation. Their implementation will require international cooperation, as well as accounting for the potential for in situ phenotypic plasticity linked with epigenetic and transcriptional changes, the empirical validation of maladaptation predictions, and innovative approaches to assessing fitness. For livestock, spatial demographic trends can be inferred from national inventories and breeder association demographic registers, offering practical alternatives to direct fitness measurements. By combining genomic insights with collaborative frameworks, we can better preserve the genetic diversity and adaptive potential of livestock, ensuring their viability in an era of rapid environmental change.

Received: 24 August 2025; Accepted: 28 August 2026;
Published online: 18 September 2026

References

1. Bernabucci, U. Climate change: impact on livestock and how can we adapt. *Anim. Front.* **9**, 3–5 (2019).
2. Rojas-Downing, M. M., Nejadhashemi, A. P., Harrigan, T. & Woznicki, S. A. Climate change and livestock: impacts, adaptation, and mitigation. *Clim. Risk Manag.* **16**, 145–163 (2017).
3. Herbut, P., Angrecka, S. & Walczak, J. Environmental parameters to assessing of heat stress in dairy cattle—a review. *Int. J. Biometeorol.* **62**, 2089–2097 (2018).
4. Hidosa, D. & Guyo, M. Climate change effects on livestock feed resources: a review. *J. Fisheries Livestock Product.* **05** (2017).
5. Tubiello, F. N., Soussana, J. F. & Howden, S. M. Crop and pasture response to climate change. *Proc. Natl. Acad. Sci. USA* **104**, 19686–19690 (2007).
6. Serranito, B. et al. Local adaptations of Mediterranean sheep and goats through an integrative approach. *Sci. Rep.* **11**, 1–17 (2021).
7. Williams, C. M. et al. Understanding evolutionary impacts of seasonality: an introduction to the symposium. *Integr. Comp. Biol.* **57**, 921–933 (2017).
8. Kawecki, T. J. & Ebert, D. Conceptual issues in local adaptation. *Ecol. Lett.* **7**, 1225–1241 (2004).
9. Daly, K. G. et al. Ancient genomics and the origin, dispersal, and development of domestic sheep. *Science* **387**, 492–497 (2025).
10. Chessa, B. et al. Revealing the history of sheep domestication using retrovirus integrations. *Science* **324**, 532–536 (2009).
11. Cao, Y.-H. et al. Historical introgression from wild relatives enhanced climatic adaptation and resistance to pneumonia in sheep. *Mol. Biol. Evolut.* https://doi.org/10.1093/molbev/msaa236 (2020).
12. Gain, C. et al. A quantitative theory for genomic offset statistics. *Mol. Biol. Evol.* **40**, msad140 (2023).
13. Hoffmann, A. A. & Sgrò, C. M. Climate change and evolutionary adaptation. *Nature* **470**, 479–485 (2011).
14. Rellstab, C., Dauphin, B. & Exposito-Alonso, M. Prospects and limitations of genomic offset in conservation management. *Evolut. Appl.* **14**, 1202–1212 (2021).
15. Capblancq, T., Fitzpatrick, M. C., Bay, R. A., Exposito-Alonso, M. & Keller, S. R. Genomic prediction of (Mal)Adaptation across current and future climatic landscapes. *Annu. Rev. Ecol. Evol. Syst.* **51**, 245–269 (2020).
16. Capblancq, T. & Forester, B. R. Redundancy analysis: a Swiss Army Knife for landscape genomics. *Methods Ecol. Evol.* **12**, 2298–2309 (2021).
17. Rochat, E., Selmoni, O. & Joost, S. Spatial areas of genotype probability: predicting the spatial distribution of adaptive genetic variants under future climatic conditions. *Divers. Distrib.* **27**, 1076–1090 (2021).
18. Bruford, M. W. et al. Prospects and challenges for the conservation of farm animal genomic resources, 2015-2025. *Front. Genet.* **6**, 314 (2015).
19. Alberto, F. J. et al. Convergent genomic signatures of domestication in sheep and goats. *Nat. Commun.* **9**, 813 (2018).
20. Pitt, D. et al. Demography and rapid local adaptation shape Creole cattle genome diversity in the tropics. *Evolut. Appl.* **18**, 105–122 (2018).
21. Gorkhali, N. A. et al. Genomic analysis identified a potential novel molecular mechanism for high-altitude adaptation in sheep at the Himalayas. *Sci. Rep.* **6**, 29963 (2016).
22. Frichot, E., Schoville, S. D., De Villemereuil, P., Gaggiotti, O. E. & François, O. Detecting adaptive evolution based on association with ecological gradients: orientation matters!. *Heredity* **115**, 22–28 (2015).
23. Selmoni, O., Vajana, E., Guillaume, A., Rochat, E. & Joost, S. Sampling strategy optimization to increase statistical power in landscape genomics: a simulation-based approach. *Mol. Ecol. Resour.* **20**, 154–169 (2020).
24. Brauning, R. Mapping of ISGC SNP chip probes. 64534502 Bytes figshare https://doi.org/10.6084/M9.FIGSHARE.8424935.V2 (2019).
25. Bolger, A. M., Lohse, M. & Usadel, B. Trimmomatic: a flexible trimmer for Illumina sequence data. *Bioinformatics* **30**, 2114–2120 (2014).
26. Li, H. Aligning sequence reads, clone sequences and assembly contigs with BWA-MEM. Preprint at https://doi.org/10.48550/ARXIV.1303.3997 (2013).
27. Picard toolkit. *Broad Institute*, *GitHub repository* (2019).
28. McKenna, A. et al. The Genome Analysis Toolkit: a MapReduce framework for analyzing next-generation DNA sequencing data. *Genome Res.* **20**, 1297–1303 (2010).
29. Garrison, E. & Marth, G. *Haplotype-based Var. detection short.-read. sequencing* https://doi.org/10.48550/arXiv.1207.3907 (2012).
30. Moreno-Romieux, C., Tortereau, F., Raoul, J. & Servin, B. High density genotypes of French Sheep populations. *Zenodo* https://doi.org/10.5281/ZENODO.237116 (2017).
31. Rochus, C. M. et al. Revealing the selection history of adaptive loci using genome-wide scans for selection: an example from domestic sheep. *BMC Genom.* **19**, 71 (2018).
32. Davenport, K. M. et al. An improved ovine reference genome assembly to facilitate in-depth functional annotation of the sheep genome. *GigaScience* **11**, 1–9 (2022).
33. Chang, C. C. et al. Second-generation PLINK: rising to the challenge of larger and richer datasets. *GigaScience* **4**, 7 (2015).
34. Frichot, E., Mathieu, F., Trouillon, T., Bouchard, G. & François, O. Fast and efficient estimation of individual ancestry coefficients. *Genetics* **196**, 973–983 (2014).
35. Frichot, E. & François, O. L. E. A. An R package for landscape and ecological association studies. *Methods Ecol. Evol.* **6**, 925–929 (2015).
36. Zheng, X. et al. A high-performance computing toolset for relatedness and principal component analysis of SNP data. *Bioinformatics* **28**, 3326–3328 (2012).

37. Dray, S. & Dufour, A.-B. The ade4 package: implementing the duality diagram for ecologists. *J. Stat. Soft*. **22**, (2007).
38. Paradis, E. & Schliep, K. ape 5.0: an environment for modern phylogenetics and evolutionary analyses in R. *Bioinformatics* **35**, 526–528 (2019).
39. Paradis, E. *Analysis of Phylogenetics and Evolution with R* (Springer New York, New York, NY, 2012). https://doi.org/10.1007/978-1-4614-1743-9.
40. Bhatia, G., Patterson, N., Sankararaman, S. & Price, A. L. Estimating and interpreting F_{ST}: the impact of rare variants. *Genome Res.* **23**, 1514–1521 (2013).
41. Fick, S. E. & Hijmans, R. J. WorldClim 2: new 1-km spatial resolution climate surfaces for global land areas. *Int. J. Climatol.* **37**, 4302–4315 (2017).
42. New, M., Lister, D., Hulme, M. & Makin, I. A high-resolution data set of surface climate over global land areas. *Clim. Res.* **21**, 1–25 (2002).
43. Dormann, C. F. et al. Collinearity: a review of methods to deal with it and a simulation study evaluating their performance. *Ecography* **36**, 27–46 (2013).
44. Forester, B. R., Lasky, J. R., Wagner, H. H. & Urban, D. L. Comparing methods for detecting multilocus adaptation with multivariate genotype–environment associations. *Mol. Ecol.* **27**, 2215–2233 (2018).
45. Caye, K., Jumentier, B., Lepeule, J. & François, O. LFMM 2: fast and accurate inference of gene-environment associations in genome-wide studies. *Mol. Biol. Evol.* **36**, 852–860 (2019).
46. Storey, J. D. A direct approach to false discovery rates. *J. R. Stat. Soc. Ser. B Stat. Methodol.* **64**, 479–498 (2002).
47. Borcard, D., Gillet, F. & Legendre, P. Canonical ordination. in *Numerical Ecology with R* 203–297 (Springer International Publishing, Cham, 2018). https://doi.org/10.1007/978-3-319-71404-2_6.
48. Gain, C. & François, O. LEA 3: factor models in population genetics and ecological genomics with R. *Mol. Ecol. Resour.* **21**, 2738–2748 (2021).
49. Oksanen, J. et al. vegan: community Ecology Package. 2.6-8 https://doi.org/10.32614/CRAN.package.vegan (2001).
50. Kijas, J. W. et al. Linkage disequilibrium over short physical distances measured in sheep using a high-density SNP chip. *Anim. Genet.* **45**, 754–757 (2014).
51. Garcia-Moreno, A. et al. Functional enrichment analysis of regulatory elements. *Biomedicines* **10** (2022).
52. Reijnders, M. J. M. F. & Waterhouse, R. M. Summary visualizations of gene ontology terms with GO-Figure!. *Front. Bioinform.* **1**, 638255 (2021).
53. Gougherty, A. V., Keller, S. R. & Fitzpatrick, M. C. Maladaptation, migration and extirpation fuel climate change risk in a forest tree species. *Nat. Clim. Chang.* **11**, 166–171 (2021).
54. Steane, D. A. et al. Genome-wide scans detect adaptation to aridity in a widespread forest tree species. *Mol. Ecol.* **23**, 2500–2513 (2014).
55. Funk, W. C., McKay, J. K., Hohenlohe, P. A. & Allendorf, F. W. Harnessing genomics for delineating conservation units. *Trends Ecol. Evolut.* **27**, 489–496 (2012).
56. Kassambara, A. & Mundt, F. factoextra: Extract and Visualize the Results of Multivariate Data Analyses. 1.0.7 https://doi.org/10.32614/CRAN.package.factoextra (2016).
57. Meehl, G. A. et al. Context for interpreting equilibrium climate sensitivity and transient climate response from the CMIP6 Earth system models. *Sci. Adv.* **6**, eaba1981 (2020).
58. Bi, D. et al. Configuration and spin-up of ACCESS-CM2, the new generation Australian Community Climate and Earth System Simulator Coupled Model. *J. South. Hemisph. Earth Syst. Sci.* **70**, 225–251 (2020).
59. Petrie, R. et al. Coordinating an operational data distribution network for CMIP6 data. *Geosci. Model Dev.* **14**, 629–644 (2021).
60. Meinshausen, M. et al. The shared socio-economic pathway (SSP) greenhouse gas concentrations and their extensions to 2500. *Geosci. Model Dev.* **13**, 3571–3605 (2020).
61. Arnholt, A. T. & Evans, B. BSDA: Basic Statistics and Data Analysis. 12 https://doi.org/10.32614/CRAN.package.BSDA (2006).
62. Velazco, S. J. E., Rose, M. B., De Marco Jr, P., Regan, H. M. & Franklin, J. How far can I extrapolate my species distribution model? Exploring shape, a novel method. *Ecography* **2024**, e06992 (2024).
63. Fitzpatrick, M. C. & Keller, S. R. Ecological genomics meets community-level modelling of biodiversity: Mapping the genomic landscape of current and future environmental adaptation. *Ecol. Lett.* **18**, 1–16 (2015).
64. Ellis, N., Smith, S. J. & Pitcher, C. R. Gradient forests: calculating importance gradients on physical predictors. *Ecology* **93**, 156–168 (2012).
65. Anselin, L. Local Indicators of Spatial Association—LISA. *Geogr. Anal.* **27**, 93–115 (1995).
66. Li, X. & Anselin, L. rgeoda: R Library for Spatial Data Analysis. 0.0.10-14 https://doi.org/10.32614/CRAN.package.rgeoda (2021).
67. R. Core Team. R: a language and environment for statistical computing. Vienna: R Foundation for Statistical Computing. (2024).
68. Vajana, E. ellios84/IMAGE-Sheep: R scripts for population and landscape genomic analyses. *Zenodo* https://doi.org/10.5281/ZENODO.21310609 (2026).
69. Metzger, M. J. et al. A high-resolution bioclimate map of the world: a unifying framework for global biodiversity research and monitoring. *Glob. Ecol. Biogeogr.* **22**, 630–638 (2013).
70. Kijas, J. W. et al. Genome-wide analysis of the world's sheep breeds reveals high levels of historic mixture and strong recent selection. *PLoS Biol.* **10**, e1001258 (2012).
71. Coelho, M. T. P., Diniz-Filho, J. A. & Rangel, T. F. A parsimonious view of the parsimony principle in ecology and evolution. *Ecography* **42**, 968–976 (2019).
72. Frichot, E., Schoville, S. D., Bouchard, G. & François, O. Testing for associations between loci and environmental gradients using latent factor mixed models. *Mol. Biol. Evolution* **30**, 1687–1699 (2013).
73. Miyachi, Y., Miyazawa, T. & Ogawa, Y. HNF1A mutations and beta cell dysfunction in diabetes. *IJMS* **23**, 3222 (2022).
74. Li, J., Mukiibi, R., Wang, Y., Plastow, G. S. & Li, C. Identification of candidate genes and enriched biological functions for feed efficiency traits by integrating plasma metabolites and imputed whole genome sequence variants in beef cattle. *BMC Genom.* **22**, 823 (2021).
75. Fan, B., Du, Z.-Q. & Rothschild, M. F. The Hepatocyte nuclear factor-1 alpha (HNF1A) gene is associated with fatness and loin muscle area in the pig. *Animal* **4**, 1619–1627 (2010).
76. Wang, D. et al. Expression and tumor-promoting effect of tyrosine phosphatase receptor type N (PTPRN) in human glioma. *Front Oncol.* **11**, 676287 (2021).
77. Wong, A. & Alejandro, E. U. Post translational modification regulation of transcription factors governing pancreatic β-cell identity and functional mass. *Front. Endocrinol*. **16** (2025).
78. Constantin, S. et al. Protein tyrosine phosphatase receptors N and N2 control pituitary melanotroph development and POMC expression. *Endocrinology* **165**, bqae076 (2024).
79. Tomati, V. et al. High-throughput screening identifies FAU protein as a regulator of mutant cystic fibrosis transmembrane conductance regulator channel. *J. Biol. Chem.* **293**, 1203–1217 (2018).
80. van Marle-Köster, E. & Visser, C. Unintended consequences of selection for increased production on the health and welfare of livestock. *Arch. Anim. Breed.* **64**, 177–185 (2021).
81. Morell Miranda, P., Soares, A. E. R. & Günther, T. Demographic reconstruction of the Western sheep expansion from whole-genome sequences. *G3: Genes, Genomes, Genet.* **13**, jkad199 (2023).

82. Siepielski, A. M. et al. Precipitation drives global variation in natural selection. *Science* **355**, 959–962 (2017).
83. Di Civita, M. et al. Exploring climate adaptation in European Merino sheep: a landscape genomics approach. *Animal* **20**, 101728 (2026).
84. Wiener, P. et al. Whole-genome sequence data suggest environmental adaptation of ethiopian sheep populations. *Genome Biol. Evol.* **13**, evab014 (2021).
85. Chen, Z.-H. et al. Whole-genome sequence analysis unveils different origins of European and Asiatic mouflon and domestication-related genes in sheep. *Commun. Biol.* **4**, 1307 (2021).
86. Niu, Y. Whole-genome sequencing identifies functional genes for environmental adaptation in Chinese sheep. (2024).
87. Yang, J. et al. Whole-genome sequencing of native sheep provides insights into rapid adaptations to extreme environments. *Mol. Biol. Evol.* **33**, 2576–2592 (2016).
88. Bertolini, F. et al. Genome-wide patterns of homozygosity provide clues about the population history and adaptation of goats. *Genet. Selection Evolut.* **50**, 59 (2018).
89. Wiedemar, N. & Drögemüller, C. A 1.8-kb insertion in the 3′-UTR of RXFP2 is associated with polledness in sheep. *Anim. Genet.* **46**, 457–461 (2015).
90. Ahbara, A. et al. Genome-wide variation, candidate regions and genes associated with fat deposition and tail morphology in Ethiopian indigenous sheep. *Front. Genet*. **9**, (2019).
91. He, Q. et al. Maternal methyl-donor micronutrient supplementation during pregnancy promotes skeletal muscle differentiation and maturity in newborn and weaning pigs. *Front. Nutr.* **7**, 1–12 (2020).
92. Lotterhos, K. E. The paradox of adaptive trait clines with nonclinal patterns in the underlying genes. *Proc. Natl. Acad. Sci. USA* **120**, e2220313120 (2023).
93. Lv, F.-H. et al. Adaptations to climate-mediated selective pressures in sheep. *Mol. Biol. Evol.* **31**, 3324–3343 (2014).
94. Lind, B. M. & Lotterhos, K. E. The accuracy of predicting maladaptation to new environments with genomic data. *Mol. Ecol. Resour.* e14008 https://doi.org/10.1111/1755-0998.14008 (2024).
95. Ciani, E. et al. On the origin of European sheep as revealed by the diversity of the Balkan breeds and by optimizing population-genetic analysis tools. *Genet. Select. Evol.* **52**, 25 (2020).
96. Lachmuth, S., Capblancq, T., Prakash, A., Keller, S. R. & Fitzpatrick, M. C. Novel genomic offset metrics integrate local adaptation into habitat suitability forecasts and inform assisted migration. *Ecol. Monogr.* **94**, e1593 (2024).
97. Scaramuzzi, R. & Martin, G. The importance of interactions among nutrition, seasonality and socio-sexual factors in the development of hormone-free methods for controlling fertility. *Reprod. Domest. Anim.* **43**, 129–136 (2008).
98. Passamonti, M. M. et al. The quest for genes involved in adaptation to climate change in ruminant livestock. *Animals* **11**, 26 (2021).
99. Francisco, T. et al. Genomic signatures of climate-driven (mal) adaptation in an iconic conifer, the English yew (Taxus baccata L. *Evolut. Appl.* **18**, e70160 (2025).
100. Archambeau, J. et al. Evaluating genomic offset predictions in a forest tree with high population genetic structure. *Am. Naturalist* **207**, 389–414 (2026).
101. Lind, B. M. et al. How useful is genomic data for predicting maladaptation to future climate? *Glob. Change Biol.* **30**, e17227 (2024).
102. CBD. 15/5. Monitoring framework for the Kunming-Montreal Global Biodiversity Framework. (2022).
103. Hoban, S. et al. DNA-based studies and genetic diversity indicator assessments are complementary approaches to conserving evolutionary potential. *Conserv Genet.* **25**, 1147–1153 (2024).

Acknowledgements

The authors wish to thank Dr. Ingrid Gosselman for Swedish sheep samples collection; the Federal States of Lower Saxony and Thuringia for providing German sheep samples; Dr. Chaz Hyseni for valuable discussions on the analysis of population genetic structure. The ovine HD BeadChip was developed under the auspices of the International Sheep Genomics Consortium and FarmIQ (http://www.farmiq.co.nz/). The authors also acknowledge the World Climate Research Programme that coordinated and promoted CMIP6 through its Working Group on Coupled Modelling. We thank the climate modelling groups for producing and making available their model output, the Earth System Grid Federation (ESGF) for archiving the data and providing access, and the multiple funding agencies who support CMIP6 and ESGF. The authors would like to dedicate this paper to the late Professor Michael W. Bruford, a champion of biodiversity conservation, and one of the first scientists to implement the landscape genomics approach to study species adaptation.

Author contributions

The paper represents the joint efforts of several research groups involved in the IMAGE project (coordinated by M.T.-B.). M.B., E.V., S.J., A.St., L.C. and P.A.M. designed the study. M.B., E.V., O.S., E.S., B.L. and L.C. curated the data. M.B. and E.V. developed the methodology. M.B., E.V., O.S. and B.L. performed formal analysis. P.A.M. provided supervision of the investigation. O.C., L.T.d.G., A.T., P.O.-t.W., M.T.P.M., A.Sc., J.J.W., S.J.H., L.F.G., G.M., E.R., U.S., A.Ä.-I., A.M.J., P.C., A.C., T.S., B.B., G.T.-K. and B.S. provided resources. M.B. and E.V. wrote the original draft. J.L.W. and P.A.M. provided critical evaluation of the first draft. All authors reviewed the manuscript.

Funding

The IMAGE project was supported by the European Union Horizon 2020 framework (Call: H2020-SFS-2015-2; grant agreement No. 677353). U.S. and E.R. were supported by the Estonian Ministry of Education and Research (grants TK215; PRG1209). Financial support to the publication of this manuscript was provided by the Linea D.3.1 (year XXXX) of the Università Cattolica del Sacro Cuore within its activities of promotion and dissemination of scientific research.

Competing interests

The authors declare no competing interests.

Additional information

Supplementary information The online version contains supplementary material available at https://doi.org/10.1038/s42003-026-10917-2.

Correspondence and requests for materials should be addressed to Elia Vajana.

Peer review information *Communications Biology* thanks the anonymous reviewers for their contribution to the peer review of this work. Primary Handling Editors: Michele Repetto. A peer review file is available.

This Article in Press is shared early to give you faster access to new research. It is citable and carries a permanent DOI. The final edited version will replace it automatically.

[1]Department of Veterinary Sciences, Università degli Studi di Messina, Messina 98168, Italy. [2]Department of Animal Science Food and Nutrition and Romeo and Enrica Invernizzi Research Center on Sustainable Dairy Production—CREI, Università Cattolica del Sacro Cuore, Piacenza 29122, Italy. [3]Institute of Biosciences and BioResources (IBBR), National Research Council (CNR), 50019 Sesto Fiorentino (Firenze), Italy. [4]Group of Geospatial Molecular Epidemiology (GEOME), Laboratory for Biological Geochemistry (LGB), School of Architecture, Civil and Environmental Engineering (ENAC), Ecole Polytechnique Fédérale de Lausanne (EPFL), 1015 Lausanne, Switzerland. [5]Carnegie Institution for Science, Stanford, CA, USA. [6]Department of Animal Production, Veterinary Faculty, Universidad Complutense de Madrid, Madrid, Spain. [7]Faculdade de Medicina Veterinária, Avenida da Universidade Técnica, 1300-477 Lisboa, Portugal. [8]CIMO, LA SusTEC, Instituto Politécnico de Bragança, Campus de Santa Apolónia, 5300-253 Bragança, Portugal. [9]School of Biosciences, Cardiff University, The Sir Martin Evans Building, Cardiff CF10 3AX, UK. [10]Departamento de Biología Funcional, Calle Julián Claveria, Universidad de Oviedo, Oviedo 33006, Spain. [11]AbacusBio Edinburgh, Roslin Innovation Centre, University of Edinburgh, EH25 9RG Edinburgh, UK. [12]Animal Breeding and Genomics, Wageningen University and Research, Wageningen 6708 PB, the Netherlands. [13]Centre for Genetic Resources, the Netherlands (CGN), Wageningen University and Research, Wageningen 6708 PB, the Netherlands. [14]Norwegian Beekeepers' Association, Kløfta 2040, Norway. [15]Department of Agricultural Sciences, Universität für Bodenkultur Wien, Vienna A-1180, Austria. [16]Department of Archaeology, Institute of History and Archaeology, University of Tartu, Tartu, Estonia. [17]Department of Zoology, Institute of Ecology and Earth Sciences, University of Tartu, Tartu, Estonia. [18]Kihnu Native Sheep Breeders Society, Manija, Estonia. [19]Department of Animal Biosciences, Faculty of Veterinary Medicine and Animal Science, Swedish University of Agricultural Sciences, Uppsala SE-75007, Sweden. [20]DiSAA – Dipartimento di Scienze Agrarie e Ambientali, Produzione, Territorio, Agroenergia, Università degli Studi di Milano, Milano, Italy. [21]Genetics and Biotechnology Research Unit, AGRIS Sardinia, Bonassai, Italy. [22]The National Institute for Agronomic Research, INR. Avenue Mohamed Belarbi Alaoui, Rabat, Morocco. [23]GenPhySE, Université de Toulouse, INRAE, Castanet Tolosan F-31326, France. [24]INRAE, AgroParisTech, Université Paris Saclay, UMR1313, Animal Genetics and Integrative Biology Domaine de Vilvert, Jouy-en-Josas Cedex 78 352, France. [25]Institute of Agriculture Biology and Biotechnology (IBBA), National Research Council of Italy (CNR), Milano 20133, Italy. [26]BioDNA Centro di ricerca sulla Biodiversità e sul DNA Antico, Università Cattolica del Sacro Cuore via Emilia Parmense 84, Piacenza 29122, Italy. ✉e-mail: eliavajana@cnr.it

IMAGE Consortium

Michèle Tixier-Boichard[27], Elisabeth Blesbois[27], Maria Bernard[27], Simon Boitard[27], Etienne Verrier[27], Antoine Doré[27], Carole Moreno[27], Michel Naves[27], Denis Laloë[27], Cyriel Paris[27], Ahmed R. A. Elbeltagy[28], Carlos Edmundo Lucero Casanova[29], Rodrigo Martínez[29], Stéphane Joost[30], Cagla Yuksel Kaya Kuyululu[31], Tessa Brinker[31], Laura Clarke[32], Peter Harrison[32], Jun Fan[32], Paul Flicek[32], Irene Hoffmann[33], Paul Boettcher[33], Roswitha Baumung[33], Steffen Weigend[34], Henner Simianer[35], Krisztina Liptói[36], Flavia Pizzi[36], Judit Barna[36], Irina Carpusca[37], Coralie Danchin[38], Delphine Duclos[38], Badr Benjelloun[39], Mouad Chentouf[39], Mustapha Ibnelbachyr[39], Hayat Lionboui[39], Julián Santiago Moreno[40], Milagros C. Esteso[40], Diego Galarza[40], Lilia Magdalena Melucci[41], Maria Rosa Lanari[41], Rudolf Preisinger[42], David Cavero Pintado[42], Peer Berg[43], Alessandra Stella[44], Paolo Cozzi[44], Eildert Groeneveld[44], Andrea Caprera[44], Waltraud Kugler[45], Dominic Moran[46], Bouda Vosough Ahmadi[46], Sipke Joost Hiemstra[47], Jack J. Windig[47], Henri Woelders[47], Harmen Doekes[47], Elzbieta Martyniuk[48], Javier Cañón[49], Susana Dunner[49], Oscar Cortés[49], Luis Telo da Gama[50], Andreia Amaral[50], Licia Colli[51], Paolo Ajmone Marsan[51], Johann Sölkner[52], Beate Berger[52], Maria Wurzinger[52], Gábor Mészáros[52], Mike McGrew[53], Hendrik-Jan Megens[54], Martien Groenen[54], Richard Crooijmans[54] & Chiara Bortoluzzi[54]

[27]Institut National de la Recherche Agronomique (INRA), Jouy-en-Josas Cedex, France. [28]Animal Production Research Institute (APRI), Cairo, Egypt. [29]Agrosavia, Bogotà, Colombia. [30]Ecole Polytechnique Fédérale de Lausanne (EPFL), Lausanne, Switzerland. [31]European Forum of Farm Animal Breeders (EFFAB), Brussels, Belgium. [32]European Molecular Biology Laboratory (EMBL), Hinxton, UK. [33]Food Agriculture Organisation (FAO), Roma, Italy. [34]Friedrich-Loeffler-Institut (FLI), Greifswald-Riems, Germany. [35]Georg-August Universität Göttingen (UGOE), Göttingen, Germany. [36]Haszonállat-génmegőrzési Központ (HáGK), Gödöllő, Hungary. [37]Inra Transfert (IT), Montpellier, France. [38]Institut de l'elevage (IDELE), Paris, France. [39]Institut National de la Recherche Agronomique du Maroc (Inra-M), Rabat, Morocco. [40]Instituto Nacional de Investigacion y Tecnologia Agraria y Alimentaria (INIA), Madrid, Spain. [41]Instituto Nacional de Tecnologia Agropecuaria (INTA), Buenos Aires, Argentina. [42]lohmann tierzucht gmbh (LTZ), Gröden-Groden, Germany. [43]Nordiskt genresurscenter (NordGen), Oslo, Norway. [44]Parco Tecnologico Padano s.r.l. (PTP), Lodi, Italy. [45]Safeguard for Agricultural Varieties in Europe (SAVE), Konstanz, Germany. [46]Scotland's Rural College (SRUC), Edinburgh, UK. [47]Stichting Wageningen Research (WR), Wageningen, the Netherlands. [48]Szkoła Główna Gospodarstwa Wiejskiego (SGGW), Warsaw, Poland. [49]Universidad Complutense de Madrid (UCM), Madrid, Spain. [50]Universidade de Lisboa (ULisboa), Lisboa, Portugal. [51]Università Cattolica del Sacro Cuore (UCSC), Piacenza, Italy.

[52]Universität für Bodenkultur (BOKU), Wien, Austria. [53]University of Edinburgh (UED), Edinburgh, UK. [54]Wageningen Universiteit (WU), Wageningen, the Netherlands.